Characterization of the detection system of SYRMA-3D

Prof. P.Delogu; Dr. V. Di Trapani

Description of the detector

- Pixirad is a direct detection photon counting device with CdTe crystalline sensor coupled to the application specific integrated circuit (ASIC) electronic;
- The ASIC, built in CMOS VLSI technology, has an active area of 30.7x24.8 mm² and is organized on a honeycomb matrix of 512x476 pixels.

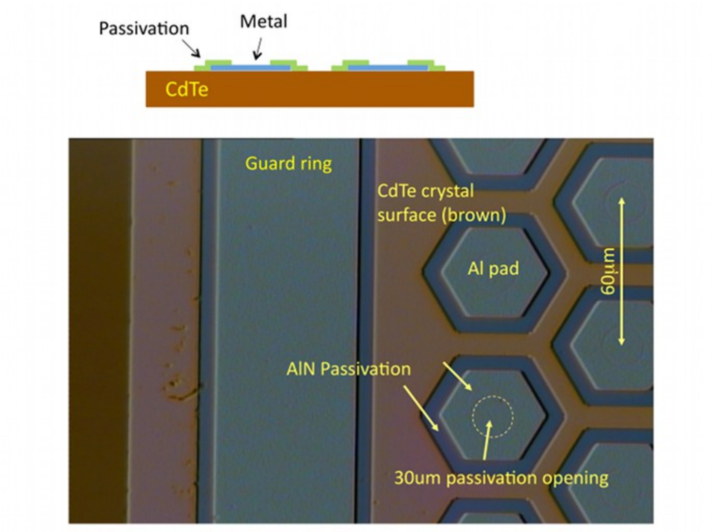

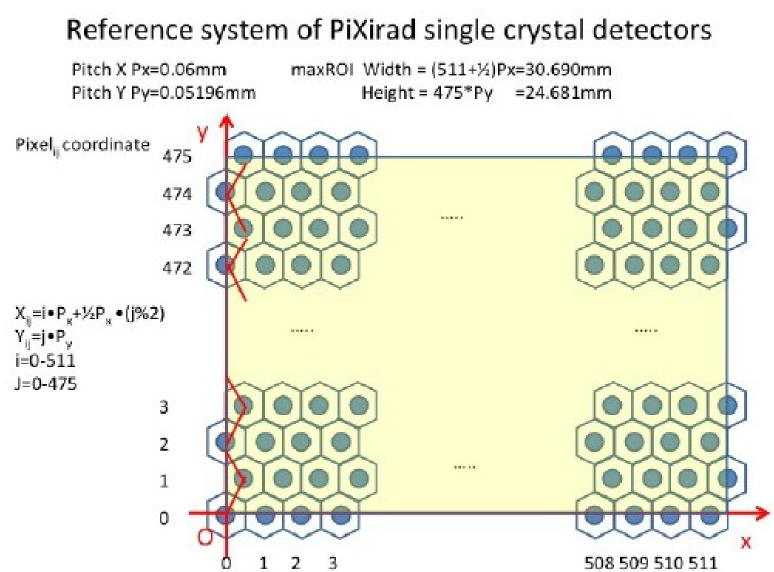

- Pixirad-8 is a 8 sensors module unit with 2M pixels, 4M counters and 25x2.5 cm² active area;

Detector: how does it works

- An incident phothon interacts with the CdTe crystal releasing its energy producing Couples of holes (h+) and charges (e-). The crystal is polarized at 400 V, so the h+ and the e- are collected by the electrodes producing an electrical signal that is treated to provide a measure of the energy released by the photon;
- Each pixel is connected to a charge amplifier that feeds two discriminators (with selectable threshold in KeV) and two 15-bit counters.

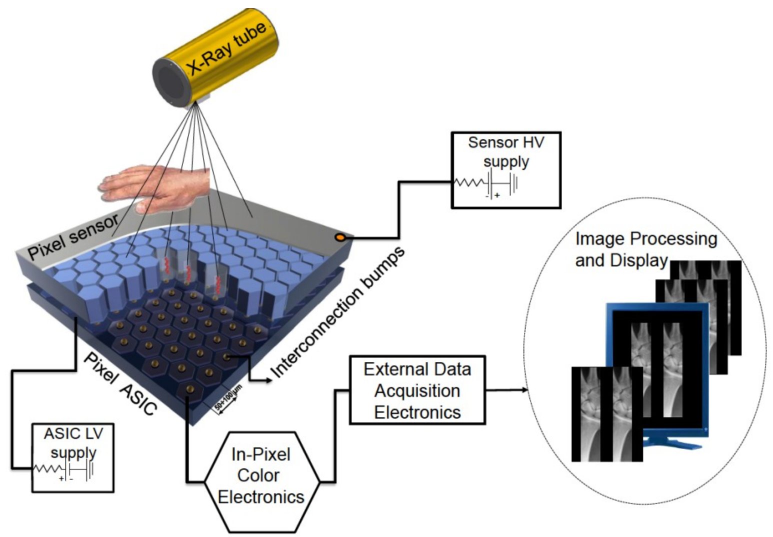

- Acquisition: 2 color reading (2 thresholds, 2 counters) or, alternatively, counting in one counter while reading the other one (dead-time free mode);
- In both modalities the selectable tresholds allow the acquisition of noise free images;

Scan acquisition workflow

1) Set-up of energy and flux to optimize the signal and the released dose;
2) Centering of the beam on the detector area;
3) Acquisition of a set of flat field images (1200);
4) CT scan (over 180 deg) in continuous rotation (4.5 deg/s) with an acquisition frame rate of 30f/s collecting 1200 projections in 40 s;
5) Each scan covers about 3 mm;
6) To cover larger volumes the scan can be repeated after traslation of the bed along the vertical axis.

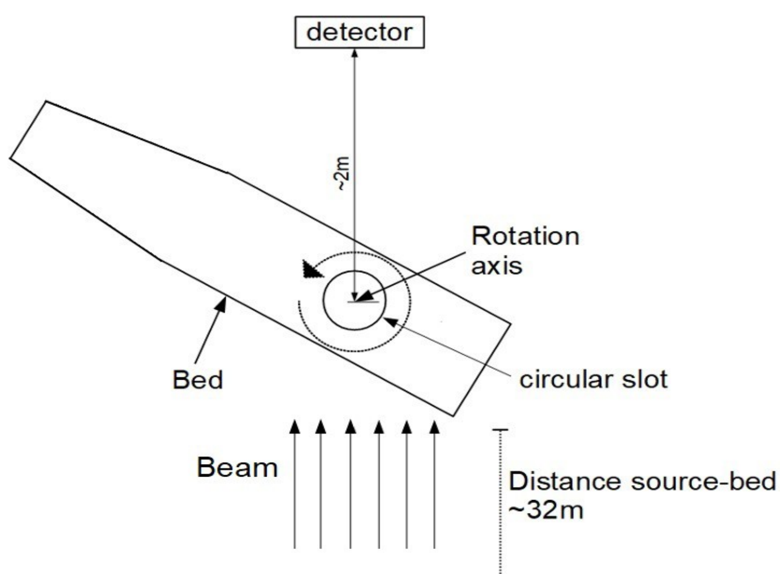

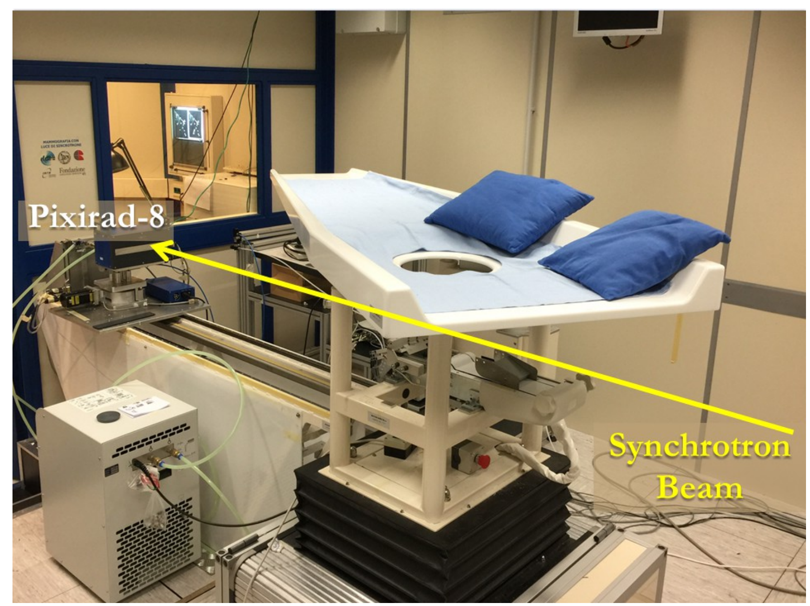

Main differences respect to an ideal detector

- The raw images are sampled into an honeycomb matrix ==> A correct visualization into digital display needs the re-sampling of the original matrix into an orthogonal one;
- The re-sampling process changes the PSF limiting the intrinsic spatial resolution of the detector;
- The charge sharing induces multiple counts from a single detected photon limiting the energy and spatial resolution;
- For energies below the K-edges of the Cd (26.7 KeV) and the Te (31.8 KeV) the fluorescence photons further degrade the spatial resolution;

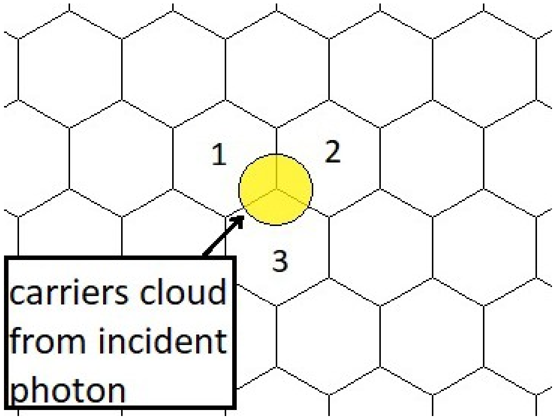

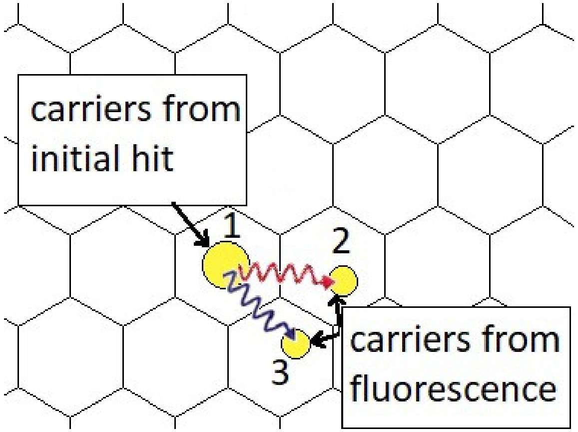

Spatial resolution (planar)

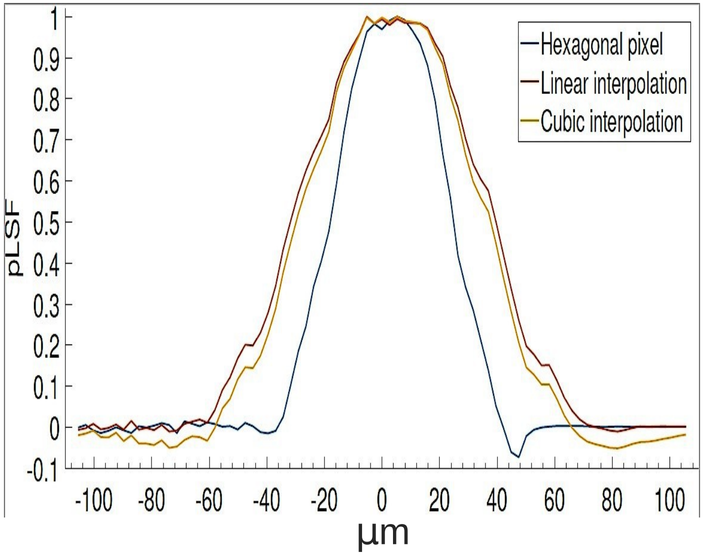

FWHM (20 KeV th 12KeV) - (38KeV th 3KeV)

- Hexagonal pixel (HeP): 42.3 (µm)
- Original resampling (OR): 67.8 (µm) - 75.9 (µm)
- Optimized resampling (OpR): 62.8 (µm)

MTF(50%) and MTF(10%) (20KeV th 12 KeV)

- Hep: 12.4 (lp/mm)- 19.5 (lp/mm)
- OR: 7.4 (lp/mm) - 13.3 (lp/mm)
- OpR: 8.4 (lp/mm) – 13.3 (lp/mm)

MTF(50%) and MTF(10%) (38KeV th 3 KeV)

- OR: 5.5 (lp/mm) – 11.0 (lp/mm)

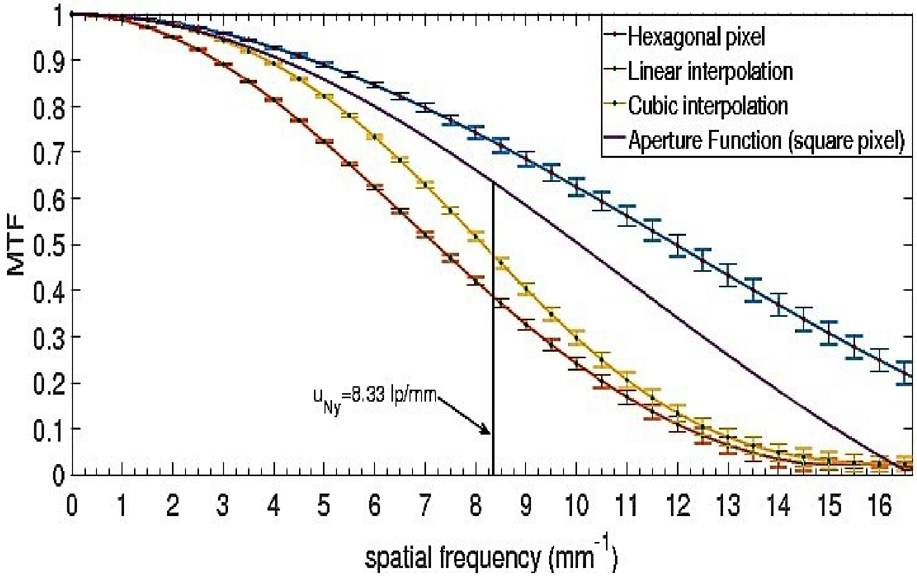

Spatial resolution (CT)

reconstructions at $60^3 \mu m^3$ voxel size

The spatial resolution of CT images depends from: 1) the spatial resolution of the 2D projections (photon energy, threshold, re-samling etc.); 2) the procedure of acquisition (continuous rotation/step, number of projections, geometry etc.); 3) the reconstruction algorithm; 4) the pre- and post- processing modulations;

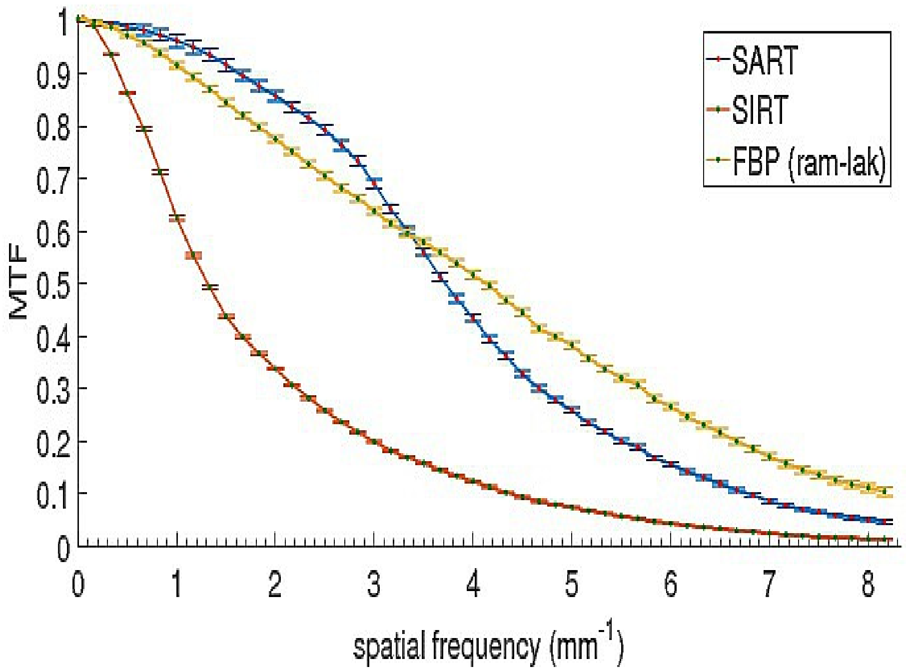

Measure performed with the thin wire method: wire at 3.2 cm from the rotation center;

algorithm	$MTF_{80\%}$ (mm^{-1})	$MTF_{50\%}$ (mm^{-1})	$MTF_{10\%}$ (mm^{-1})
FBP (ram-lak)	1.83	**4.16**	**8.17**
FBP (Shepp-Logan)	1.67	3.75	7.33
FBP (Hamming)	1.42	2.83	5.5
FBP (Hann)	1.41	2.75	5.25
SART	**2.41**	3.75	6.67
SIRT	0.66	1.33	4.33

algorithm	$FWHM_{AVG}$ (μm)	$FWHM_{radial}$ (μm)	$FWHM_{tangential}$ (μm)
FBP (ram-lak)	132 ± 1	104 ± 2	161 ± 1
FBP (Shepp-Logan)	138 ± 1	111 ± 2	165 ± 1
FBP (Hamming)	165.0 ± 0.7	146.1 ± 0.7	186 ± 1
FBP (Hann)	170.8 ± 0.7	152.8 ± 0.6	189 ± 1
SART	144.0 ± 0.9	120 ± 1	167.6 ± 0.9
SIRT	199 ± 1	169 ± 1	228 ± 1

Spatial resolution (CT)

reconstructions at $120^3 \mu m^3$ voxel size

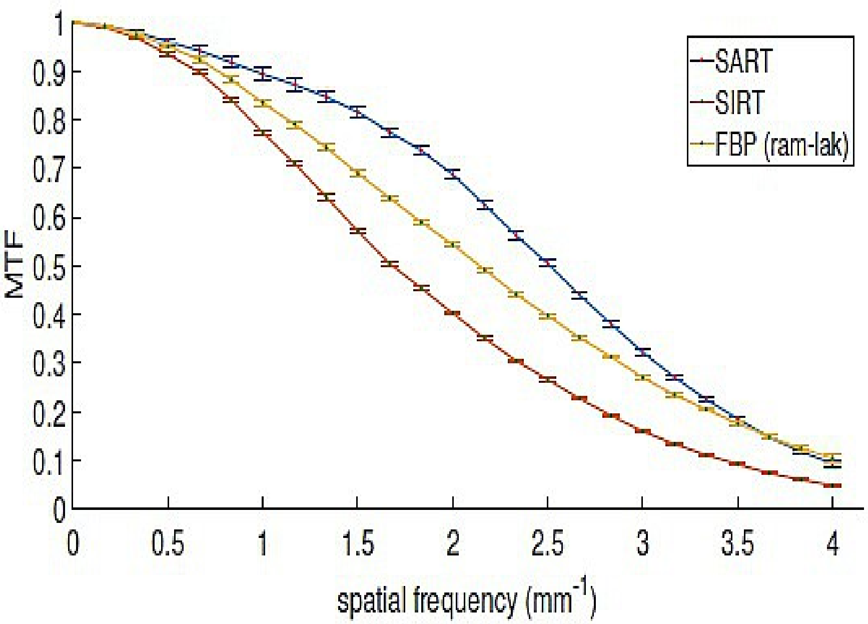

algorithm	$MTF_{80\%}$ (mm^{-1})	$MTF_{50\%}$ (mm^{-1})	$MTF_{10\%}$ (mm^{-1})
FBP (ram-lak)	1.13	2.14	**>4.16**
FBP (Shepp-Logan)	1.04	1.98	3.70
FBP (Hamming)	0.82	1.52	2.79
FBP (Hann)	0.83	1.48	2.68
SART	**1.56**	**2.51**	3.96
SIRT	0.80	1.68	3.43

algorithm	$FWHM_{AVG}$ (μm)	$FWHM_{radial}$ (μm)	$FWHM_{tangential}$ (μm)
FBP (ram-lak)	231 ± 2	223 ± 4	240 ± 3
FBP (Shepp-Logan)	245 ± 2	236 ± 4	254 ± 3
FBP (Hamming)	306.7 ± 0.7	297 ± 1	315.9 ± 0.9
FBP (Hann)	318.0 ± 0.5	309.5 ± 0.7	326.5 ± 0.8
SART	216 ± 4	204 ± 4	228 ± 3
SIRT	257 ± 2	243 ± 3	270 ± 2

Noise planar (NNPS)

The noise of planar images depends on:

- **In SD** The number N of the incident photons==> Poissonian statistic σ~ $N^{(1/2)}$
- **In FD** the charge sharing and the fluorescence (increase of the correlation in the NNPS);

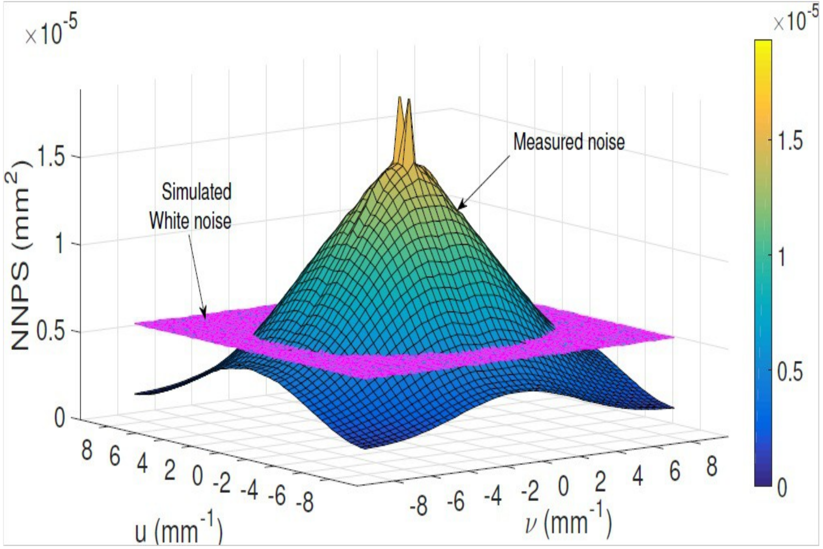

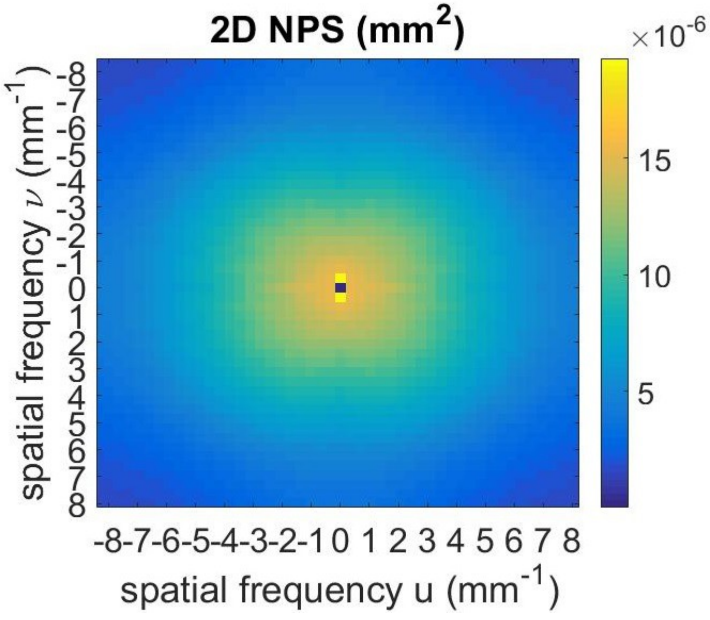

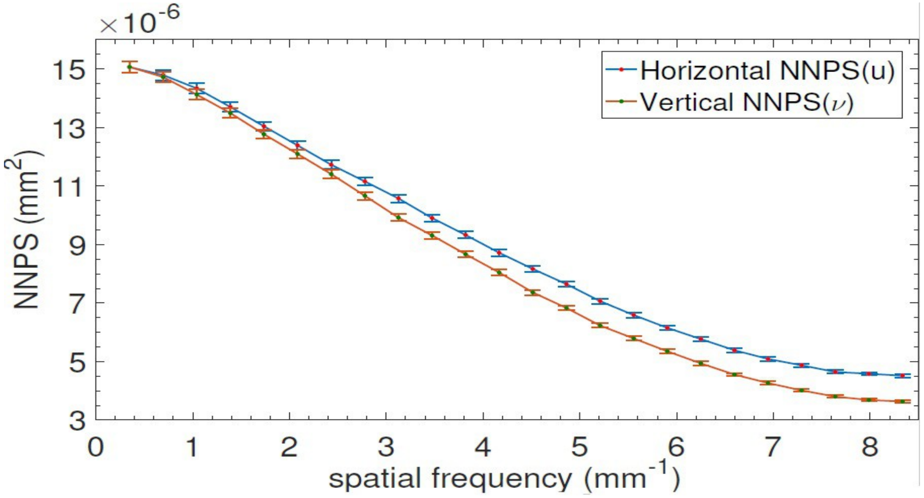

Noise CT

The noise of CT images depends on:

- The noise of the 2D projections;
- The reconstruction algorithm (FBP, FBP filters, iterative..);
- The radial distance from the center of the reconstructed image (decreases with the increase of the radial distance);

Example: 2D NNPS for images with 60^3 µm^3 voxel size

2D NNPS (FBP)

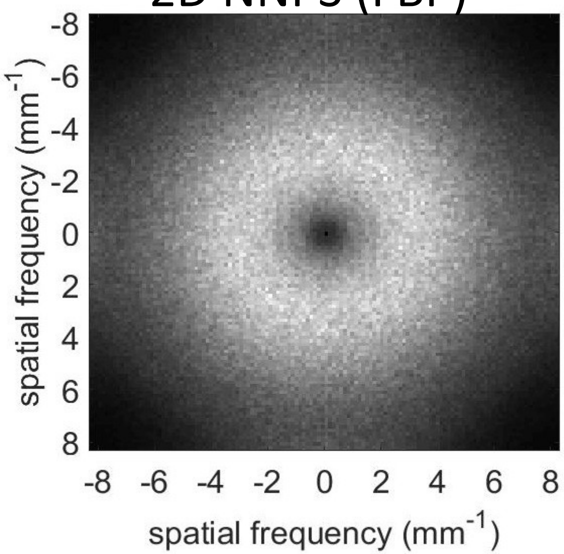

2D NNPS (SART)

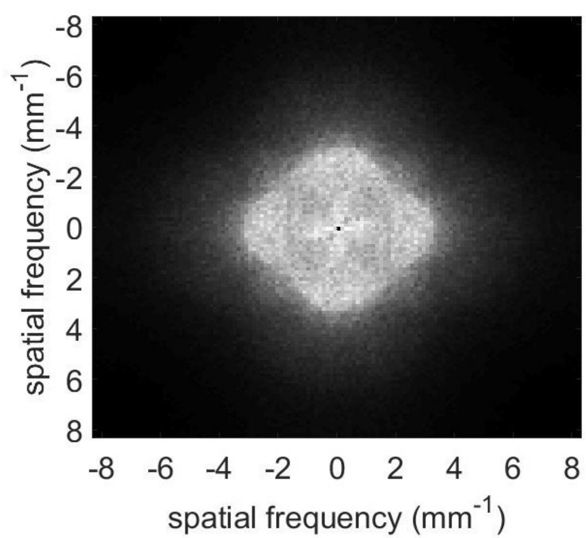

2D NNPS (SIRT)

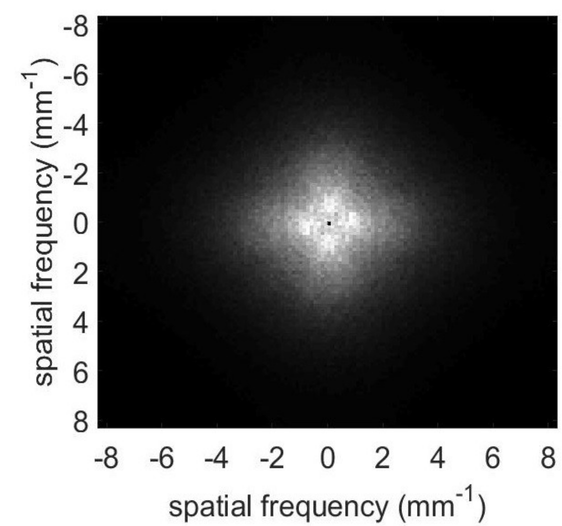

Energy resolution

Integral spectra

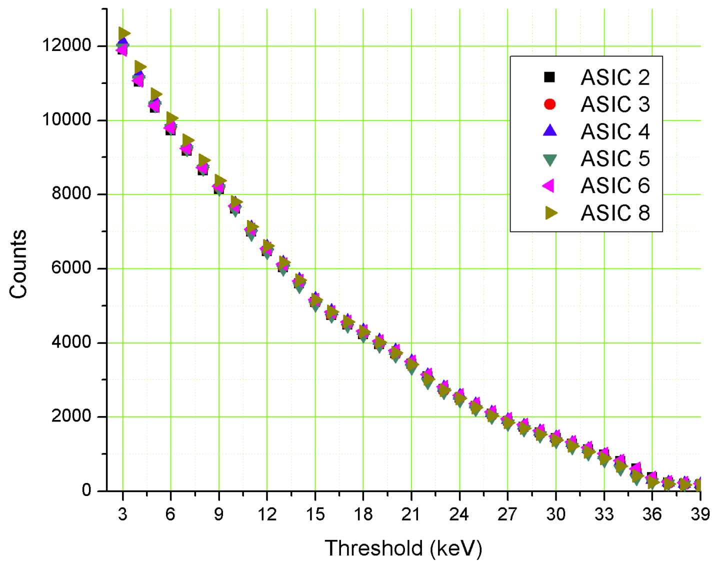

differential spectrum

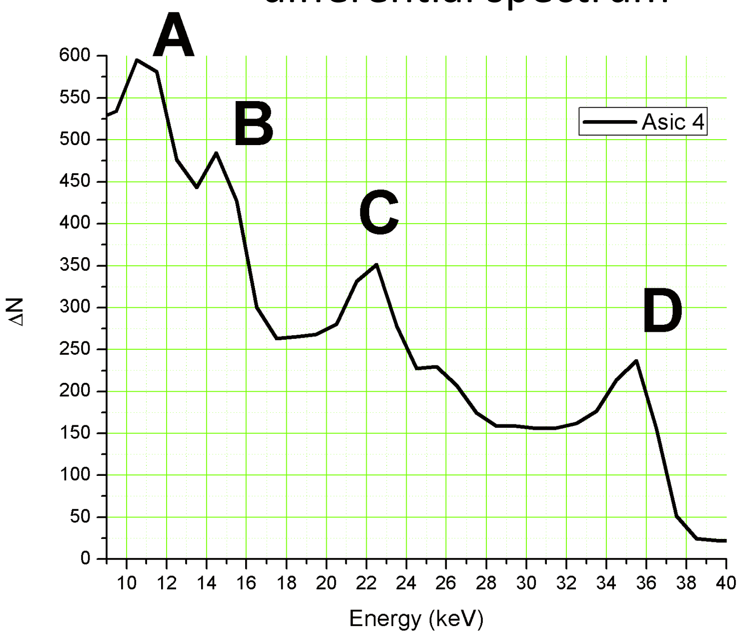

D=full energy peak (38 keV)

C= fluorescence of Cd (23 keV)

B=15 keV peak (38keV-23keV): the energy released by the primary photon which interacts with the Cd (photoelectric) reduced by the fluorescence photon detected in a different region;

A=11 keV peak (38keV-27keV): energy released by the ionization of the K-edge of the Cd;

INFN Istituto Nazionale di Fisica Nucleare

Continuous rotation 1

- The projections collected with the continuous acquisition in continuous rotation are integrated over the time 1/f where f is the frame rate of acquisition inducing a blurring over the tangential direction of the reconstructed images;

Simulation of CT with Continuous rotation: detail at 5 cm from the centre

2400 1200 800 600 400

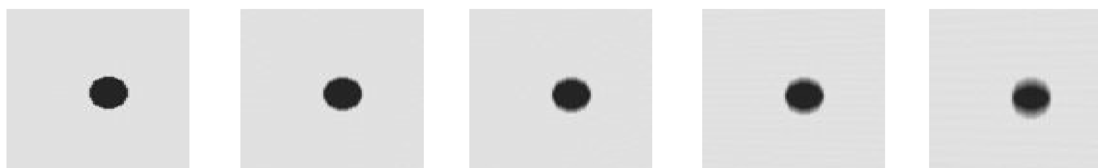

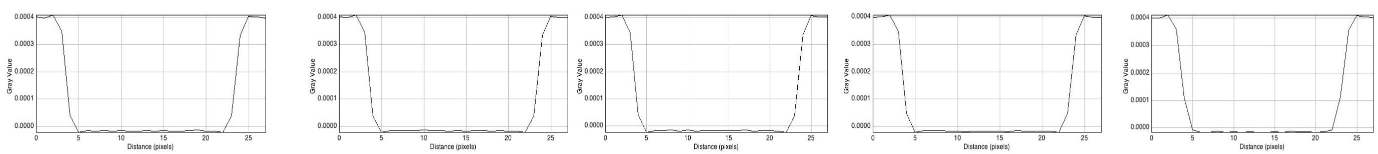

radial

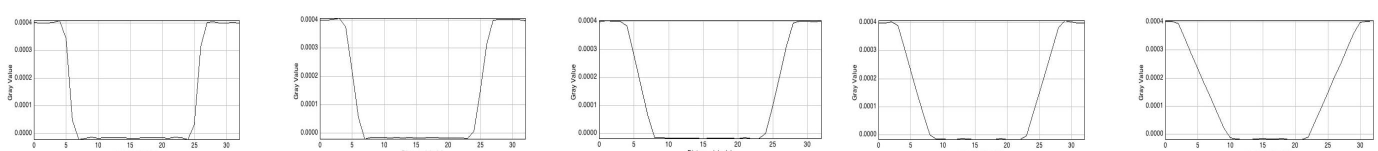

tangential

Continuous rotation 2

In presence of noise the effect of the blurring along the tangential direction is slightly masked

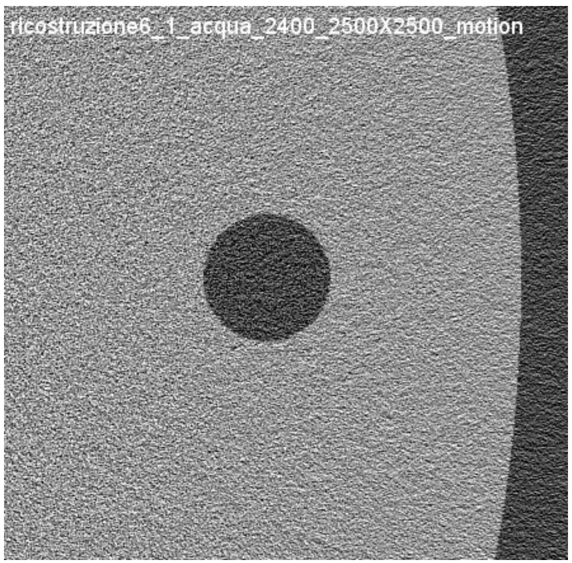

Observations: 1) during the continuous rotation the information about the phase contrast are spread over the angle of integration==> what about phase retrieval along the tangential direction?